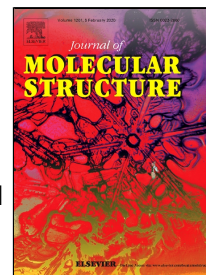


Journal Pre-proof



Synthesis of luminescent rhodium(III) cyclometalated complex by $sp^2(C)$ -S bond activation: Application as catalyst in transfer hydrogenation of ketones and live cell imaging

Puspendu Roy, Deblina Sarkar, Paramita Ghosh, Chandan Kumar Manna, Nabendu Murmu, Tapan Kumar Mondal

PII: S0022-2860(19)31633-3
DOI: <https://doi.org/10.1016/j.molstruc.2019.127524>
Reference: MOLSTR 127524

To appear in: *Journal of Molecular Structure*

Received Date: 31 October 2019
Accepted Date: 02 December 2019

Please cite this article as: Puspendu Roy, Deblina Sarkar, Paramita Ghosh, Chandan Kumar Manna, Nabendu Murmu, Tapan Kumar Mondal, Synthesis of luminescent rhodium(III) cyclometalated complex by $sp^2(C)$ -S bond activation: Application as catalyst in transfer hydrogenation of ketones and live cell imaging, *Journal of Molecular Structure* (2019), <https://doi.org/10.1016/j.molstruc.2019.127524>

This is a PDF file of an article that has undergone enhancements after acceptance, such as the addition of a cover page and metadata, and formatting for readability, but it is not yet the definitive version of record. This version will undergo additional copyediting, typesetting and review before it is published in its final form, but we are providing this version to give early visibility of the article. Please note that, during the production process, errors may be discovered which could affect the content, and all legal disclaimers that apply to the journal pertain.

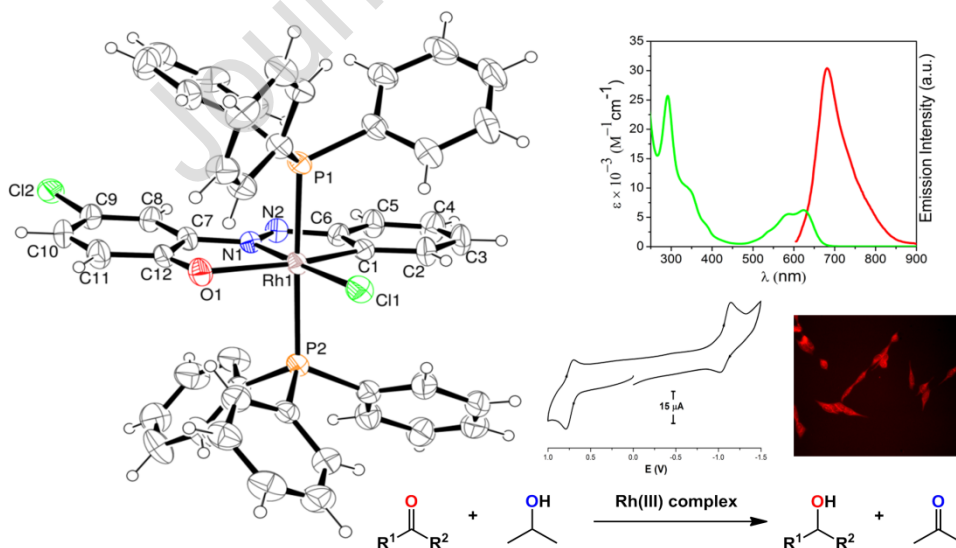
© 2019 Published by Elsevier.

Graphical Abstract

Synthesis of luminescent rhodium(III) cyclometalated complex by $sp^2(C)$ -S bond activation: Application as catalyst in transfer hydrogenation of ketones and live cell imaging

Puspendu Roy, Deblina Sarkar, Paramita Ghosh, Chandan Kumar Manna, Nabendu Murmu and Tapan Kumar Mondal

A new fluorescent Rh(III) cyclometalated complex, $[\text{Rh}(\text{PPh}_3)_2(\text{L})\text{Cl}]$ (**1**) has been synthesized via $sp^2(C)$ -S bond activation of a thioether containing azo-phenol ligand ($\text{L-SCH}_2\text{CH}_3$). The complex exhibits low energy emission band at 682 nm with high emission quantum yield ($\phi = 0.103$). In presence of the complex a bright red fluorescence image of MCF-7 cell lines is observed under fluorescence microscope. Catalytic activity of complex **1** towards transfer hydrogenation of ketones is studied.



Synthesis of luminescent rhodium(III) cyclometalated complex by $sp^2(C)$ -S bond activation: Application as catalyst in transfer hydrogenation of ketones and live cell imaging

Puspendu Roy^{a,d}, Deblina Sarkar^b, Paramita Ghosh^c, Chandan Kumar Manna^a, Nabendu Murmu^c and Tapan Kumar Mondal^{a*}

^aDepartment of Chemistry, Jadavpur University, Kolkata-700032, India.

^bDepartment of Chemistry, Bagnan College, Howrah, W.B. 711303, India.

^cDepartment of Signal Transduction and Biogenesis Amines, Chittaranjan National Cancer Institute, Kolkata- 700026, India

^dPresent address: Department of Chemistry, Netaji Nagar Day College, University of Calcutta, Kolkata – 700092, India.

Abstract

A new fluorescent Rh(III) cyclometalated complex, $[Rh(PPh_3)_2(L)Cl]$ (**1**) is synthesized via $sp^2(C)$ -S bond activation of a thioether containing azo-phenol ligand (L-SCH₂CH₃). The pseudo octahedral geometry around rhodium is confirmed by single crystal X-ray diffraction method. Cyclic voltammogram of the complex exhibits a quasi-reversible oxidation couple with $E_{1/2}$ of 0.74 V ($\Delta E = 100$ mV) along with a quasi-reversible reduction couple ($E_{1/2} = -1.18$ V, $\Delta E = 130$ mV) in acetonitrile. The complex exhibits low energy emission band at 682 nm with emission quantum yield ($\phi = 0.103$) upon excitation at 583 nm. Cytotoxicity of the complex is studied by MTT method with human breast cancer cell lines and IC_{50} value is found to 18.5 μM . In presence of the complex (10 μM) a bright red fluorescence image of MCF-7 cell lines is

observed under fluorescence microscope. Moreover, the complex acts as effective catalyst towards transfer hydrogenation of ketones.

Key words: Rhodium(III) cyclometalated complex; C-S bond activation; Luminescence property; Transfer hydrogenation; Live cell imaging; DFT calculation.

Corresponding author: Email: tapank.mondal@jadavpuruniversity.in

1. Introduction

For the last few years, cyclometalated complexes of Rh(III) and Ir(III) are widely studied because of their outstanding photochemical, photophysical and redox properties [1,2]. They have wide applications as potential photocatalysts, photosensitizers and photomolecular devices [3,4]. The luminescent Ir(III) complexes are the most researched class of materials considering their extensive use as the emitters in organic light-emitting cells and diodes [5-7], sensors [8,9] and in cellular imaging [10,11]. But, similar type of Rh(III) complexes are rarely studied because of their poor photophysical properties [12,13]. In the last decades luminescent transition metal complexes have attracted considerable interest for application in biosensing and cellular imaging study [14]. Cellular imaging offers a unique approach for visualizing morphological details inside the cell. Although polyaromatic organic chromophores are most widely used as fluorescence probes in cellular imaging, luminescent metal complexes especially with heavy transition metals are better probes for bioimaging because of their superior photophysical properties

with high photostability and relatively long life time. They also exhibit significant Stokes shifts for easy separation of excitation and emission wavelengths.

In recent years metal mediated C-S bond activation has witnessed a tremendous upsurge in catalytic reactions [15-17]. The platinum group metal mediated alkyl C(sp³)-S bond cleavage is widely studied in recent past [18-21], but metal mediated aryl C(sp²)-S bond activation and formation of cyclometalated complex is rarely studied [22-25]. Herein, we have synthesized luminescent rhodium(III) cyclometalated complex, [Rh(PPh₃)₂(L)Cl] (**1**) via aryl C(sp²)-S bond cleavage of thioether containing azo-phenol ligand (L-SCH₂CH₃). The catalytic property of the complex **1** towards transfer hydrogenation of ketones in *i*-PrOH was studied. In addition, the biocompatibility of the complex was checked with human breast cancer cell lines (MCF-7) by in vitro cytotoxicity assay using MTT. The cell bioimaging study was also carried out in MCF-7 cell lines.

2. Experimental section

2.1. Material and methods

Bis(triphenylphosphine)rhodium(I)carbonyl chloride, [Rh(PPh₃)₂(CO)Cl] and 2-aminothiophenol were purchased from Sigma Aldrich. 4-Chloro-2-((2-(ethylthio)phenyl)diazanyl)phenol (L-SCH₂CH₃) was prepared following the reported method [26]. Microanalytical data (C, H, N) were collected on PerkinElmer 2400 CHNS/O elemental analyzer. Infrared spectra were taken on a RX-1 Perkin Elmer spectrophotometer with samples prepared as KBr pellets. ¹H NMR spectra were recorded on Bruker 300 MHz instrument in CDCl₃. HRMS mass spectra were recorded on Waters (Xevo G2 Q-TOF) mass spectrometer. Electronic spectra were taken on a PerkinElmer Lambda 750 spectrophotometer. Luminescence property was measured using Shimadzu RF-6000

fluorescence spectrophotometer at rt (298 K). Cyclic voltammetric measurements were carried out using a CHI Electrochemical workstation. A platinum wire working electrode, a platinum wire auxiliary electrode and Ag/AgCl reference electrode were used in a standard three-electrode configuration. [*n*-Bu₄N][ClO₄] was used as the supporting electrolyte in acetonitrile under N₂ atmosphere with scan rate of 50 mV/s.

2.2. Synthesis of [Rh(PPh₃)₂(L)Cl] (1)

0.173 g (0.25 mmol) Rh(PPh₃)₂(CO)Cl was dissolved in 10 mL acetonitrile. To it 10 mL acetonitrile solution of 4-chloro-2-((2-(ethylthio)phenyl)diazenyl)phenol (L-SCH₂CH₃) (0.073 g, 0.25 mmol) was added and the reaction mixture was refluxed for 12 h under N₂ atmosphere to yield a deep blue solution. The solvent was then removed under reduced pressure. The dried crude product was purified by using a silica gel (mesh 60-120) column. The blue band of **1** was eluted by 50% (v/v) ethyl acetate-petroleum ether mixture. On removal of the solvent under reduced pressure the pure complex **1** was obtained as a blue solid which was further dried under vacuum. Yield, 0.140 g (63%).

Anal. Calc. for C₄₈H₃₇Cl₂N₂OP₂Rh: C, 64.52; H, 4.17; N, 3.13%; Found: C, 64.69; H, 4.09; N, 3.07%. IR data (KBr, cm⁻¹): 1410 ν(N=N). ¹H NMR data (CDCl₃, ppm): 7.97 (1H, s), 7.63 (2H, d, J = 7.2), 7.21-7.56 ppm (34H, m). UV-vis in acetonitrile (nm) (ε, M⁻¹cm⁻¹): 627 (6390), 583 (5637), 535 (sh.), 388 (sh.), 346 (sh.), 291 (25627). λ_{em} in acetonitrile (λ_{ex} = 583 nm): 682 nm. HRMS *m/z*, 893.7215 (M-H⁺). Cyclic voltammetry (in acetonitrile, scan rate 50 mV/s): E_{1/2}, 0.74 V (ΔE = 100 mV) and E_{1/2}, -1.18 V (ΔE = 130 mV).

2.3. X-ray crystallography

Single crystals of **1** were obtained by slow diffusion of *n*-hexane into dichloromethane solution of the complex. X-ray data were collected using an automated Bruker AXS Kappa smart Apex-II diffractometer equipped with an Apex-II CCD area detector using a fine focus sealed tube as the radiation source of graphite monochromated Mo K α radiation ($\lambda = 0.71073 \text{ \AA}$). Details of crystal analyses, data collection and structure refinement are summarized in Table 1. Reflection data were recorded using the ω scan technique. The structure was solved and refined by full-matrix least-squares techniques on F^2 using the SHELX-97 [27]. The absorption corrections were done by multi-scan (SHELXTL program package) and all the data were corrected for Lorentz, polarization effect. Hydrogen atoms were included in the refinement process as per the riding model.

2.4. Theoretical study

All calculations were performed with Gaussian 09 program package [28] with the support of the Gauss View visualization program. Full geometry optimizations were carried out using the density functional theory (DFT) method at the B3LYP level for the compound [29,30]. All elements except rhodium were assigned 6-31+G(d) basis set. The LanL2DZ basis set with effective core potential (ECP) set of Hay and Wadt was used for rhodium atom [31-33]. Vertical electronic excitations based on B3LYP optimized geometries were computed using the time-dependent density functional theory (TDDFT) formalism [34-36] in acetonitrile using conductor-like polarizable continuum model (CPCM) [37-39].

2.5. Procedure for catalytic transfer hydrogenation

In a typical experiment the ketone (3 mmol), KOH (0.1 mmol), and rhodium(III) complex (**1**) (0.006 mmol) were added to 10 mL of *i*-PrOH, and the mixture was stirred at 80 °C in an inert atmosphere. The reaction was then monitored at various time intervals by the use of GC. After

the reaction was complete, *i*-PrOH was removed on a rotary evaporator, and the resulting semisolid was extracted with diethyl ether (5×10 mL). The extract was passed through a short column of silica gel. The column was washed with ~ 100 mL of diethyl ether. All the eluates from the column were mixed, and the solvent from the mixture was evaporated off on a rotary evaporator. The resulting residue was dissolved in 2-3 mL of hexane. Conversions were determined by GC instrument equipped with a flame ionization detector (FID) using a HP-5 column of 30 m length, 0.53 mm diameter and 5.00 μm film thickness. The column, injector and detector temperatures were 200, 250 and 250 $^{\circ}\text{C}$ respectively. The carrier gas was N_2 (UHP grade) at a flow rate of 30 mL/min. The injection volume of sample was 2 μL . The alcohols were identified by GC using undecane as an internal standard and each of the catalytic run was performed three times.

2.6. In vitro cell imaging

2.6.1. Cell Survivability assay

Human breast cancer cell lines MCF-7 were evaluated for cytotoxicity with rhodium(III) complex, $[\text{Rh}(\text{PPh}_3)_2(\text{L})\text{Cl}]$ (**1**). MCF-7 cell lines were obtained from National centre for cell science, Pune, India and maintained in Minimum Essential Media Earle's (MEM) (Gibco, life technologies) supplemented with 10% Fetal Bovine Serum (FBS) (Gibco, life technologies, USA) and stored at 37 $^{\circ}\text{C}$ in a humidified incubator under 5% CO_2 atmosphere. Cells were seeded in 96-well plates at a density of 5×10^3 cells per well and cultured in CO_2 incubator for 24 h. The cells were treated with increasing doses complex concentrations (5, 10, 20, 25, 30, 50, 75, 100) μM , along with control. Complex **1** was dissolved in DMSO but the final concentration of DMSO while treatment of cells was maintained below 1%. After treatment for 24 h, Methyl tetrazolium dye (MTT) (5 mg/ml) solution was added to each well (10 μL /well). The plates were

incubated in the dark at 37 °C for 2 h. To each well 100 μ L DMSO was added and allowed to stand for 1 h in a vortex shaker. Cell viability determination was studied by recording absorbance at 570 nm for each well using a microplate reader (Tecan, infinite M200). Untreated cells were served as 100% viable. Linearly fitted plot between complex concentration and O.D value at 570 nm was generated for determination of IC₅₀ value of the free receptor. Concentration of the complex resulting in 50% death after 24 h treatment was obtained as the IC₅₀ value.

2.6.2. Live cell imaging

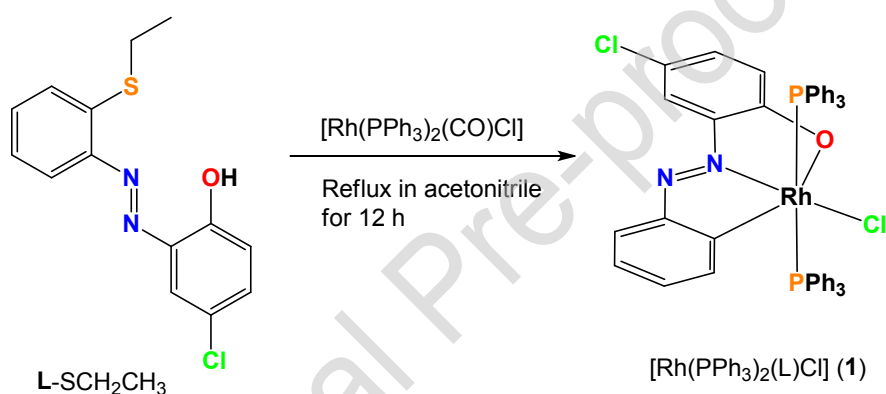
Cultured cells were then grown on 22×22 mm glass cover slip placed on the bottom of six well plates and treated with 10 μ M of complex for 12 h. The selected dose (10 μ M) was less than LD₅₀ which was found to be 18.53 μ M. After 12 h, media were discarded and 500 μ l methanol added, kept for 15 min for fixation. Finally the cells were washed with 0.5 % Phosphate buffer saline Tween (PBST) twice and then with 1×PBS thrice. The cover slips were mounted on slides using glycerol. The slides were observed under fluorescent microscope (Leica DM4000 B, Germany) under 20X magnification.

3. Results and discussion

3.1. Synthesis and formulation

The thioether containing tridentate O, N, S donor ligand, 4-chloro-2-((2-(ethylthio)phenyl)diazanyl)phenol (L-SCH₂CH₃) was synthesized as air stable red solid by diazo-coupling of 2-(ethylthio)benzenamine with 4-chlorophenol following the reported method [26]. Stoichiometric reaction between L-SCH₂CH₃ and Rh(PPh₃)₂(CO)Cl in acetonitrile under refluxing condition yielded deep blue product (scheme 1). The complex was thoroughly characterized by several spectroscopic techniques. ¹H NMR spectrum of the complex was taken

CDCl_3 . The significant observation in the spectrum of the complex is the disappearance of $\text{S}-\text{CH}_2\text{CH}_3$ resonances due to cleavage of C-S bond. The structure of the complex is unambiguously determined by single crystal X-ray diffraction method. Interestingly, instead of cleavage of $\text{sp}^3(\text{C})-\text{S}$ bond [40], the $\text{sp}^2(\text{C})-\text{S}$ bond is cleaved followed by removal of SCH_2CH_3 group and a direct $\text{Rh}-\text{C}(\text{aryl})$ bond formation is taking place in the complex. Due to desulfurization the modified ligand is coordinated as tridentate fashion to rhodium centre through azo-N, phenolic-O and aryl-C atom.



Scheme 1. Synthesis of $[\text{Rh}(\text{PPh}_3)_2(\text{L})\text{Cl}]$ (**1**) by C-S bond cleavage of $\text{L}-\text{SCH}_2\text{CH}_3$

3.2. Crystal structure

The geometry of the complex was ascertained by single crystal X-ray diffraction method. Single crystals were grown by slow diffusion of dichloromethane solution of the complex into hexane at rt. The X-ray crystallographic data collection and refinement parameters of **1** are given in Table 1. Selected bond lengths and bond angles are summarized in Table 2. ORTEP plot of the molecular structure with the atomic numbering scheme for **1** is shown in Fig. 1. The rhodium atom adopts a distorted octahedral geometry and is coordinated by two PPh_3 groups in *trans*

positions of the octahedron, the modified chelating ligand (L) coordinated through phenolic-O, azo-N and aryl-C atoms. The vacant position of the square plane is occupied by chlorine atom. The deviation of the rhodium coordination sphere from the ideal octahedron is because of the small bite angles of the five membered chelate rings (Rh1-C1-C6-N2-N1) (78.97(17)°) and (Rh1-N1-C7-C12-O1) (80.25(14)°). The Rh-P (Rh1-P1, 2.4085(13) and Rh1-P2, 2.4288(14) Å), Rh-Cl (Rh1-Cl1, 2.4108(13) Å) and Rh-C (Rh1-C1, 2.023(4) Å) bond distances are found as expected for similar rhodium phosphine complexes [25, 41-43]. The azo, N-N bond distance in the complex is found to be elongated (N1-N2, 1.304(5) Å) supporting $d\pi(\text{Rh}^{\text{III}}) \rightarrow \pi^*(\text{N}=\text{N})$ back donation.

3.3. Absorption and emission spectra

The UV-vis spectrum of the complex **1** in acetonitrile exhibits two closed by low energy bands at 627 nm ($\epsilon = 6390 \text{ M}^{-1}\text{cm}^{-1}$) and 583 nm ($\epsilon = 5637 \text{ M}^{-1}\text{cm}^{-1}$) along with a shoulder at 535 nm. In addition a high energy sharp band is observed at 291 nm ($\epsilon = 25627 \text{ M}^{-1}\text{cm}^{-1}$) along with the shoulder at 346 nm and 388 nm. Upon excitation at 583 nm in acetonitrile the complex exhibits very strong emission spectrum with λ_{max} at 682 nm (Fig. 2). The emission quantum yield (ϕ) of the complex is found to be 0.103. Lifetime data of the emission decay curve was deconvoluted with respect to the lamp profile. The observed emission decay fits with bi-exponential profile with $\chi^2 = 1.106$ (Fig. 3). We have used mean fluorescence lifetime ($\tau_f = a_1\tau_1 + a_2\tau_2$, where a_1 and a_2 are relative amplitude of decay process) to study the excited state stability of the complex. The emission lifetime of the complex is found to be 2.26 ns.

3.4. DFT and TDDFT calculation

The full geometry of the complex **1** was optimized by DFT method in singlet ground state using the B3LYP correlation functional. The optimized bond parameters for complex **1** are given in

Table 2. The calculated bond distances and angles are well correlated with the X-ray crystal structure data.

The contour plots of selected molecular orbitals are given in Fig. 4. Energy and % of composition is summarized in Table 3. HOMO of the complex is found to be 93% $\pi(L)$ character and concentrated on phenolate moiety of the ligand along with very minor contribution of $d\pi(Rh)$ orbital. HOMO-1 and HOMO-2 have mixed $d\pi(Rh)$, $\pi(L)$ and $p\pi(Cl)$ character. The low energy unoccupied molecular orbital (LUMO) has 93% $\pi^*(L)$ character with major contribution of $\pi^*(N=N)$ orbital. The significant contribution of $d\pi(Rh)$ along with $\pi(PPh_3)$ orbitals is found to be in LUMO+1 and LUMO+2 of the complex.

To interpret the electronic spectra, singlet-singlet vertical electronic excitations were calculated by TDDFT/CPCM method in acetonitrile. Strong HOMO to LUMO transition is found to be at 593 nm ($f = 0.1683$) having ILCT character. One low energy weak transition corresponding to HOMO \rightarrow LUMO+1 transition (LMCT/ILCT character) at 515 nm is observed (Table 4). The high energy transition of the complex at 326 nm ($f = 0.3676$) corresponding to the experimental band at 291 nm.

3.5. Electrochemistry

The electrochemical behavior of the complex was investigated by cyclic voltammetry (CV) in presence of $[n-Bu_4N][ClO_4]$ in acetonitrile at scan rate 50 mVS⁻¹. In the potential window 1.5 to -1.5 V complex **1** exhibits one quasi-reversible oxidation couple with $E_{1/2}$ of 0.74 V ($\Delta E = 100$ mV) along with one quasi-reversible reduction couple ($E_{1/2} = -1.18$ V, $\Delta E = 130$ mV) positive and negative to the reference electrode respectively (Ag/AgCl) (Fig. 5). The redox behavior of the complexes is interpreted by DFT study. HOMO of the complex has 93% $\pi(L)$ character with major contribution of phenolate moiety of the ligand, so the oxidation of the complex is assigned

as oxidation of phenolate moiety to form phenoxy radical [19,44]. LUMO of the complex has 93% ligand character with major contribution of $\pi^*(N=N)$ orbital. Therefore the reduction of the complex is assigned as the reduction of azo(N=N) bond to form azo anion radical ($L/L^{\bullet-}$) as expected.

3.6. Catalytic transfer hydrogenation

The transfer hydrogenation is an important and efficient reaction in organic synthesis. So far many rhodium(III) complexes were used as effective catalysts for transfer hydrogenation reactions [21,43], which encourage us to use our synthesized Rh(III) cyclometalated complex as catalyst for the transfer hydrogenation of ketones.

Initially to optimize the reaction condition, catalytic efficiency of complex **1** for the conversion of acetophenone to 1-phenylethanol was tested in *i*-PrOH with the variation of catalyst to substrate ratio (C:S), reaction time and different bases and the results are summarized in Table 5. The conversion was found to be effective in presence of strong base KOH in comparison to Na_2CO_3 , CH_3COONa or KO^tBu . Again, to understand the catalytic efficiency of the complex **1**, different catalyst:substrate (C:S) ratios were tested in the transfer hydrogenation of acetophenone in *i*-PrOH/KOH. It is found that the conversion is maximum in C:S ratio of 1:300. With the variation of C:S ratio to 1:400 to 1:1500, the reaction still proceeds but a sharp decrease in rate of conversion is observed for C:S ratio 1:600 to 1:1500. The conversion is excellent with appreciable turnover number (TON) when the C:S ratio is 1:500 and hence this C:S ratio is the best choice for catalytic transfer hydrogenation reactions for complex **1**. Again, to understand the effect of the catalyst, the reactions were also carried out in absence of the Rh(III) complex but no significant catalytic conversions were observed. A series of ketones were screened in transfer hydrogenation reaction using the optimum condition, C:S ratio of 1:500 and KOH as base. The

results are summarized in Table 6. The maximum conversions were observed for 1-(4-chlorophenyl)ethanone (99%), acetophenone (98%), 1-(*p*-tolyl)ethanone (98%) and *p*-nitroacetophenone (98%). The conversions of other acetophenones were found to be in the range of 91-97%. The catalytic efficiency of the present rhodium(III) cyclometalated complex is found to be very competitive with the reported transfer hydrogenation catalysts [45-47].

3.7. Cell bio-imaging

A yellow coloured tetrazolium salt MTT (3-(4,5-dimethylthiazol-2-yl)-2,5-diphenyltetrazolium bromide) was used to quantify mammalian cell survivability and proliferation. Mitochondria of viable cells reduce it to a non-fluorescent insoluble formazan, purple colour dye. Thus the degree of viability of cells can be determined by measuring the absorbance of the purple coloured solution at 570 nm. MTT experiment establishes that the rhodium(III) complex has moderate toxicity on human breast cancer cell line MCF-7 (Fig. 6). The IC_{50} value of the complex on MCF-7 cell line is found to be 18.53 μM . The chosen dose was taken to be lower than the IC_{50} value of the complex at 10 μM concentration. Upon incubation of MCF-7 cells with the complex causes a striking red fluorescence in the intracellular region (Fig. 7). This observation clearly indicates that the present luminescent rhodium(III) complex may be used as biomarker for fluorescence imaging. Through bright field images, it is observed that the treated cells do not show any distinct or visible morphological changes indicating that the cells are viable in the used concentration of the complex.

4. Conclusion

Herein, we have synthesized a new fluorescent Rh(III) cyclometalated complex, $[Rh(PPh_3)_2(L)Cl]$ (**1**) via C-S bond activation of a thioether containing azo-phenol ligand (L-SCH₂CH₃). The distorted octahedral geometry of the complex is confirmed by X-ray structure.

The complex exhibits a quasi-reversible oxidation couple ($E_{1/2} = 0.74$ V, $\Delta E = 100$ V) along with quasi-reversible reduction peak at $E_{1/2} = -1.18$ V ($\Delta E = 130$ mV). The complex exhibits low energy emission band at 682 nm with high emission quantum yield ($\phi = 0.103$). Cytotoxicity of the complex is studied by MTT method with human breast cancer cell lines (MCF-7) and IC_{50} value is found to be $18.5 \mu\text{M}$. In presence of the complex ($10 \mu\text{M}$) a bright red fluorescence image of MCF-7 cell lines is observed under fluorescence microscope. The complex exhibits efficient catalytic activity towards transfer hydrogenation of ketones.

Acknowledgment

Financial supports received from the Science and Engineering Research Board (SERB), New Delhi, India (EEQ/2018/000266) is gratefully acknowledged. P. Roy and R. Naskar are thankful to UGC, New Delhi, India for fellowship. C. K. Manna is grateful to RUSA 2.0 programme for fellowship.

Supplementary materials

Crystallographic data for the structure of **1** has been deposited with the Cambridge Crystallographic Data center, CCDC No. 1496012. Copies of this information may be obtained free of charge from the Director, CCDC, 12 Union Road, Cambridge CB2 1EZ, UK (e-mail: deposit@ccdc.cam.ac.uk or [www:http://www.ccdc.cam.ac.uk](http://www.ccdc.cam.ac.uk)).

Reference

- [1] W.L. Su, Y.C. Yu, M.C. Tseng, S.P. Wang, W.L. Huang, Dalton Trans. (2007) 3440-3449.
- [2] L.S. Forster, J.V. Rund, Inorg. Chem. Commun. 6 (2003) 78-81.
- [3] M. Graf, V. Gancheva, M. Thesen, H. Krüger, P. Mayer, K. Sünkel, Inorg. Chem. Commun. 11 (2008) 231-234.

- [4] W.L. Su, Y.C. Yu, M.C. Tseng, S.P. Wang, W.L. Huang, Dalton Trans. (2007) 3440-3449.
- [5] Y. You, W. Nam, Chem. Soc. Rev. 41 (2012) 7061-7084.
- [6] C.-H. Lin, Y.-Y. Chang, J.-Y. Hung, C.-Y. Lin, Y. Chi, M.-W. Chung, C.-L. Lin, P.-T. Chou, G.-H. Lee, C.-H. Chang, W.-C. Lin, Angew. Chem., Int. Ed. 50 (2011) 3182-3186.
- [7] Y.-J. Yuan, J.-Y. Zhang, Z.-T. Yu, J.-Y. Feng, W.-J. Luo, J.-H. Ye, Z.-G. Zou, Inorg. Chem. 51 (2012) 4123-4133.
- [8] Y. You, S. Cho, W. Nam, Inorg. Chem. 53 (2014) 1804-1815.
- [9] J. Liu, Y. Liu, Q. Liu, C. Li, L. Sun, F. Li, J. Am. Chem. Soc. 133 (2011) 15276-15279.
- [10] S. Mandal, D. K. Poria, D. K. Seth, P. S. Ray, P. Gupta, Polyhedron. 73 (2014) 12-21.
- [11] C. Li, M. Yu, Y. Sun, Y. Wu, C. Huang, F. Li, J. Am. Chem. Soc. 133 (2011) 11231-11239.
- [12] S.K. Leung, K. Y. Kwok, K. Y. Zhang, K. K.-W. Lo, Inorg. Chem. 49 (2010) 4984-4995.
- [13] A.C. Komor, C.J. Schneider, A.G. Weidmann, J.K. Barton, J. Am. Chem. Soc. 134 (2012) 19223-19233.
- [14] R. Tan, D. Song, Organometallics. 30 (2011) 1637-1645.
- [15] S.G. Modha, V.P. Mehta, E.V. Van der Eycken, Chem. Soc. Rev. 42 (2013) 5042-5055.
- [16] S. Mandal, N. Paul, P. Banerjee, T.K. Mondal, S. Goswami, Dalton Trans. 39 (2010) 2717-2726.
- [17] M. Albrecht, Chem. Rev. 110 (2010) 576-623.
- [18] U. Das, T. Ghorui, B. Adhikary, S. Roy, S. Pramanik, K. Pramanik, Dalton Trans., 44 (2015) 8625-8639.
- [19] S. Biswas, P. Roy, T.K. Mondal, J. Mol. Struct. 1142 (2017) 110-115.
- [20] K. Pramanik, U. Das, B. Adhikary, D. Chopra, H. Stoeckii-Evans, Inorg. Chem., 47 (2008) 529-534.

- [21] P. Roy, C.K. Manna, R. Naskar, T.K. Mondal, *Polyhedron* 158 (2019) 208-214.
- [22] M. Neurock, R. A. van Santen, *J. Am. Chem. Soc.* 116 (1994) 4427-4439.
- [23] N.F. Ho, T.C.W. Mak, T.-Y. Luh, *J. Organomet. Chem.* 317 (1986) 28-30.
- [24] M. Tiecco, L. Testaferri, M. Tingoli, D. Chianelli, *Tetrahedron Lett.* 23 (1982) 4629-4632.
- [25] S. Acharya, P. Bandyopadhyay, P. Das, S. Biswas, A.N. Biswas, *J. Organomet. Chem.* 866 (2018) 13-20.
- [26] P. Roy, A. Sau Mondal, A.K. Mondal, T.K. Mondal, *J. Organomet. Chem.* 828 (2017) 1-9.
- [27] SHELXS97: G.M. Sheldrick, *SHELX97*, Programs for Crystal Structure Analysis (release 97-2); University of Göttingen: Göttingen, Germany (1997).
- [28] Gaussian 09, Revision D.01, M.J. Frisch, G.W. Trucks, H.B. Schlegel, G.E. Scuseria, M.A. Robb, J.R. Cheeseman, G. Scalmani, V. Barone, B. Mennucci, G.A. Petersson, H. Nakatsuji, M. Caricato, X. Li, H.P. Hratchian, A.F. Izmaylov, J. Bloino, G. Zheng, J.L. Sonnenberg, M. Hada, M. Ehara, K. Toyota, R. Fukuda, J. Hasegawa, M. Ishida, T. Nakajima, Y. Honda, O. Kitao, H. Nakai, T. Vreven, J. A. Montgomery, Jr., J.E. Peralta, F. Ogliaro, M. Bearpark, J.J. Heyd, E. Brothers, K.N. Kudin, V.N. Staroverov, R. Kobayashi, J. Normand, K. Raghavachari, A. Rendell, J.C. Burant, S.S. Iyengar, J. Tomasi, M. Cossi, N. Rega, J.M. Millam, M. Klene, J.E. Knox, J.B. Cross, V. Bakken, C. Adamo, J. Jaramillo, R. Gomperts, R.E. Stratmann, O. Yazyev, A.J. Austin, R. Cammi, C. Pomelli, J.W. Ochterski, R.L. Martin, K. Morokuma, V.G. Zakrzewski, G.A. Voth, P. Salvador, J.J. Dannenberg, S. Dapprich, A.D. Daniels, Ö. Farkas, J.B. Foresman, J.V. Ortiz, J. Cioslowski, D.J. Fox, Gaussian, Inc., Wallingford CT (2009).
- [29] A.D. Becke, *J. Chem. Phys.* 98 (1993) 5648-5652.
- [30] C. Lee, W. Yang, R.G. Parr, *Phys. Rev. B* 37 (1988) 785-789.

- [31] P.J. Hay, W.R. Wadt, *J. Chem. Phys.* 82 (1985) 270-283.
- [32] W.R. Wadt, P.J. Hay, *J. Chem. Phys.* 82 (1985) 284-298.
- [33] P.J. Hay, W.R. Wadt, *J. Chem. Phys.* 82 (1985) 299-310.
- [34] R. Bauernschmitt, R. Ahlrichs, *Chem. Phys. Lett.* 256 (1996) 454-464.
- [35] R.E. Stratmann, G.E. Scuseria, M.J. Frisch, *J. Chem. Phys.* 109 (1998) 8218-8224.
- [36] M.E. Casida, C. Jamorski, K.C. Casida, D.R. Salahub, *J. Chem. Phys.* 108 (1998) 4439-4449.
- [37] V. Barone, M. Cossi, *J. Phys. Chem. A* 102 (1998) 1995-2001.
- [38] M. Cossi, V. Barone, *J. Chem. Phys.* 115 (2001) 4708-4717.
- [39] M. Cossi, N. Rega, G. Scalmani, V. Barone, *J. Comput. Chem.* 24 (2003) 669-681.
- [40] P. Roy, R. Naskar, C.K. Manna, T.K. Mondal, *J. Mol. Struct.* 1198 (2019) 126932.
- [41] S. Roy, S. Pramanik, T. Ghorui, S. Dinda, S.S. Patra, K. Pramanik, *New J. Chem.* 42 (2018) 5548-5555.
- [42] S. Baksi, R. Acharyya, S. Dutta, A.J. Blake, M.G.B. Drew, S. Bhattacharya, *J. Organomet. Chem* 692 (2007) 1025-1032.
- [43] S. Basu, S. Dutta, M.G.B. Drew, S. Bhattacharya, *J. Organomet. Chem.* 691 (2006) 3581-3588.
- [44] S. Jana, A.K. Pramanik, C.K. Manna, T.K. Mondal, *Polyhedron* 150 (2018) 118-125.
- [45] A. Mannu, G. Vlahopoulou, C. Kubis, H.-J. Drexler, *J. Organomet. Chem.* 885 (2019) 59-64.
- [46] M. Ramesh, G. Venkatachalam, *J. Organomet. Chem.* 880 (2019) 47-55.
- [47] P.-G. Echeverria, C. Ferard, P. Phandavath, V. Ratovelomanana-Vidal, *Catal. Commun.* 62 (2015) 95-99.

Table 1. Crystallographic data for [Rh(Cl)(PPh₃)₂(L)] (1)

| | |
|---|---|
| Formula | C ₄₈ H ₃₇ Cl ₂ N ₂ OP ₂ Rh |
| Formula Weight | 893.55 |
| Crystal System | <i>Monoclinic</i> |
| Space group | <i>P2₁/c</i> |
| a, b, c [Å] | 12.6327(5), 19.1782(7), 18.7752(6) |
| β | 109.558(2) |
| V [Å ³] | 4286.3(3) |
| Z | 4 |
| D(calc) [g/cm ³] | 1.385 |
| Mu(MoKa) [/mm] | 0.636 |
| F(000) | 1824 |
| Crystal Size [mm] | |
| Temperature (K) | 293(2) |
| Radiation [Å] | 0.71073 |
| θ(Min-Max) [°] | 2.01- 27.25 |
| Dataset (h; k; l) | -15 and 15; -24 and 23; -24 and 24 |
| Total, Unique Data, R(int) | 66181, 9459, 0.0880 |
| Observed data [I > 2σ(I)] | 5716 |
| Nref, Npar | 9459, 506 |
| R1, wR2[I > 2σ(I)] | 0.0666; 0.1576 |
| GOF | 1.031 |
| Largest diff. Peak/hole, (e Å ⁻³) | -1.290; 1.617 |

Table 2. Some selected bond distances (Å) and angles (°) of [Rh(Cl)(PPh₃)₂(L)] (1)

| Bonds(Å) | X-ray | Calc. |
|------------|------------|---------|
| Rh1-N1 | 1.972(3) | 2.006 |
| Rh1-C1 | 2.023(4) | 2.016 |
| Rh1-O1 | 2.220(3) | 2.278 |
| Rh1-P1 | 2.4085(13) | 2.457 |
| Rh1-P2 | 2.4288(14) | 2.457 |
| Rh1-Cl1 | 2.4108(13) | 2.445 |
| N1-N2 | 1.304(5) | 1.277 |
| O1-C12 | 1.327(6) | 1.298 |
| N1-C7 | 1.416(6) | 1.391 |
| C1-C6 | 1.423(6) | 1.429 |
| Angles(°) | | |
| N1-Rh1-C1 | 78.97(17) | 79.252 |
| N1-Rh1-O1 | 80.25(14) | 78.009 |
| C1-Rh1-O1 | 159.19(16) | 157.262 |
| N1-Rh1-P1 | 90.36(11) | 93.349 |
| C1-Rh1-P1 | 91.27(14) | 92.094 |
| O1-Rh1-P1 | 89.98(10) | 89.231 |
| N1-Rh1-P2 | 95.60(11) | 93.350 |
| C1-Rh1-P2 | 91.40(14) | 92.094 |
| O1-Rh1-P2 | 89.50(10) | 89.233 |
| O1-Rh1-Cl1 | 100.83(10) | 102.099 |
| N1-Rh1-Cl1 | 178.62(11) | 179.890 |
| C1-Rh1-Cl1 | 99.97(14) | 100.638 |

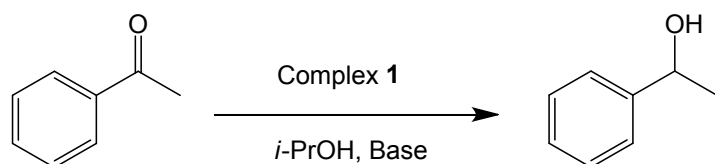
Table 3. Energy and compositions of some selected molecular orbitals of **1**

| MO | Energy | % Composition | | | |
|---------|--------|---------------|------------------|----|----|
| | | Rh | PPh ₃ | L | Cl |
| LUMO+5 | -0.55 | 01 | 95 | 03 | 0 |
| LUMO+4 | -0.60 | 01 | 98 | 0 | 01 |
| LUMO+3 | -0.61 | 01 | 94 | 05 | 0 |
| LUMO+2 | -0.84 | 29 | 47 | 20 | 04 |
| LUMO+1 | -1.70 | 33 | 54 | 08 | 05 |
| LUMO | -2.27 | 04 | 03 | 93 | 0 |
| HOMO | -4.98 | 05 | 02 | 93 | 0 |
| HOMO-1 | -5.78 | 35 | 03 | 27 | 36 |
| HOMO-2 | -5.91 | 11 | 34 | 26 | 29 |
| HOMO-3 | -6.20 | 14 | 12 | 53 | 21 |
| HOMO-4 | -6.26 | 09 | 40 | 51 | 0 |
| HOMO-5 | -6.36 | 06 | 38 | 42 | 14 |
| HOMO-6 | -6.62 | 02 | 76 | 12 | 09 |
| HOMO-7 | -6.69 | 01 | 97 | 02 | 01 |
| HOMO-8 | -6.70 | 02 | 92 | 03 | 03 |
| HOMO-9 | -6.84 | 02 | 82 | 12 | 04 |
| HOMO-10 | -6.86 | 10 | 78 | 10 | 02 |

Table 4. The experimental absorption bands and the electronic transitions calculated with the TDDFT/B3LYP/CPCM method for complex **1**

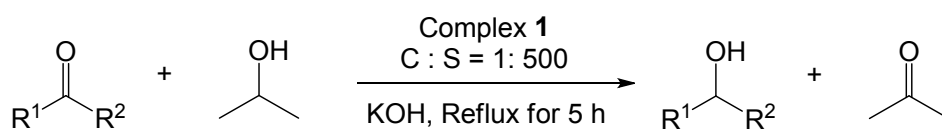
| λ (nm) | E (eV) | Osc. Strength (f) | Key excitations | Character | $\lambda_{\text{expt.}}$ (nm) (ϵ ($\text{M}^{-1}\text{cm}^{-1}$)) |
|-------------------|--------|----------------------|--------------------|-----------|--|
| 593.3 | 2.0896 | 0.1683 | (97%)HOMO→LUMO | ILCT | 627 (6390) |
| 515.2 | 2.4064 | 0.0108 | (93%)HOMO→LUMO+1 | LMCT/ILCT | 583 (5637) |
| 414.1 | 2.9939 | 0.0104 | (96%)HOMO-1→LUMO | MLCT | 535 (sh) |
| 375.4 | 3.3028 | 0.0366 | (67%)HOMO-3→LUMO | ILCT | 388 (sh) |
| 365.0 | 3.3971 | 0.0641 | (82%)HOMO-4→LUMO | ILCT | |
| 352.5 | 3.5175 | 0.0625 | (62%)HOMO-2→LUMO+3 | ILCT | 346 (sh) |
| 337.8 | 3.6702 | 0.1418 | (69%)HOMO-3→LUMO+3 | ILCT | |
| 326.2 | 3.8009 | 0.3676 | (72%)HOMO-5→LUMO | ILCT | 291 (25627) |

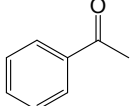
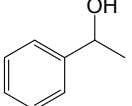
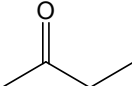
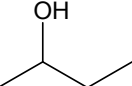
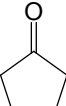
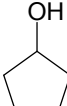
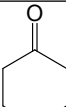
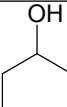
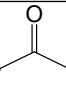
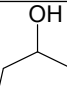
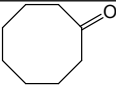
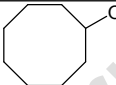
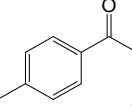
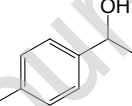
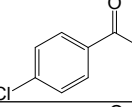
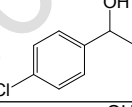
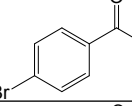
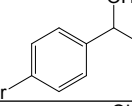
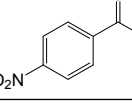
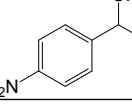
Table 5. Effect of C:S ratio, base and reaction time on the transfer hydrogenation of acetophenone^a



| Entry | C:S ratio | Base | Time (h) | Conversion ^b (%) | TON ^c |
|-------|-----------|---------------------------------|----------|-----------------------------|------------------|
| 1 | 1:300 | KOH | 3 | 67 | 202 |
| 2 | 1:300 | KOH | 4 | 81 | 244 |
| 3 | 1:300 | KOH | 5 | 99 | 296 |
| 4 | 1:300 | KOH | 7 | 99 | 297 |
| 5 | 1:300 | KOH | 10 | 99 | 297 |
| 6 | 1:300 | NaOH | 5 | 96 | 287 |
| 7 | 1:300 | Na ₂ CO ₃ | 5 | 53 | 158 |
| 8 | 1:300 | CH ₃ COONa | 5 | 43 | 128 |
| 9 | 1:300 | KO ^t Bu | 5 | 67 | 200 |
| 10 | 1:400 | KOH | 5 | 98 | 392 |
| 11 | 1:500 | KOH | 5 | 98 | 488 |
| 12 | 1:600 | KOH | 5 | 84 | 506 |
| 13 | 1:800 | KOH | 5 | 69 | 548 |
| 14 | 1:1000 | KOH | 5 | 43 | 428 |
| 15 | 1:1500 | KOH | 5 | 25 | 398 |

^aReaction condition: acetophenone (3 mmol), complex **1** (10-2 μ mol), catalyst:KOH 1:4 in *i*-PrOH (10 mL) at 80 °C; ^bConversions were determined by GC with undecane as an internal standard and were reported mean values of three runs; ^cTurnover number (TON) = mole of product/mol of catalyst.

Table 6. Transfer hydrogenation of ketones using complex **1**^a

| Entry | Ketones | Alcohols | Conversion (%) ^b | TON ^c |
|-------|---|---|-----------------------------|------------------|
| 1 |  |  | 98 | 488 |
| 2 |  |  | 94 | 472 |
| 3 |  |  | 95 | 476 |
| 4 |  |  | 96 | 479 |
| 5 |  |  | 94 | 468 |
| 6 |  |  | 92 | 458 |
| 7 |  |  | 98 | 491 |
| 8 |  |  | 99 | 493 |
| 9 |  |  | 97 | 493 |
| 10 |  |  | 98 | 492 |

^aExperimental condition: reactions were carried out at 80 °C, ketone (3 mmol), Rh(III) complex (0.2 mol%), KOH (0.1 mmol), *i*-PrOH (10 mL); ^bConversions were determined by GC with undecane as an internal standard and were reported mean values of three runs; ^cTurnover number (TON) = mole of product/mol of catalyst

Figure captions

Fig. 1. ORTEP plot with 35% ellipsoidal probability of **1**

Fig. 2. UV-vis (—) and emission (—) spectra of complex **1** in acetonitrile

Fig. 3. Life time decay profile of **1** (●●●) ($\lambda_{\text{ex}} = 490$ nm) and prompt (■■■) in acetonitrile

Fig. 4. Contour plots of selected molecular orbitals of **1**

Fig. 5. Cyclic voltammogram of **1** in acetonitrile with respect to Ag/AgCl reference electrode ([*n*-Bu₄N][ClO₄] was used as the supporting electrolyte)

Fig. 6. MTT assay of complex **1** on MCF-7 cell line

Fig. 7. (a) Fluorescence image, (b) bright field image and (c) merged image of human breast cancer cell lines (MCF-7) in presence of complex **1**

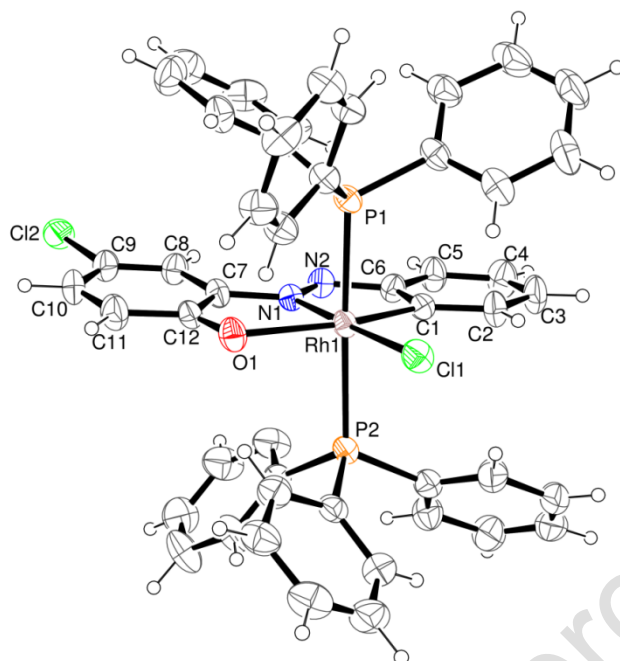


Fig. 1

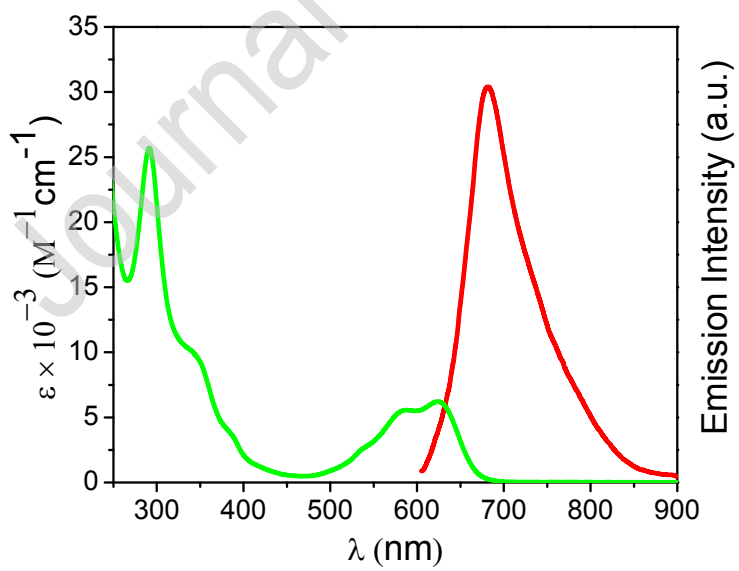


Fig. 2

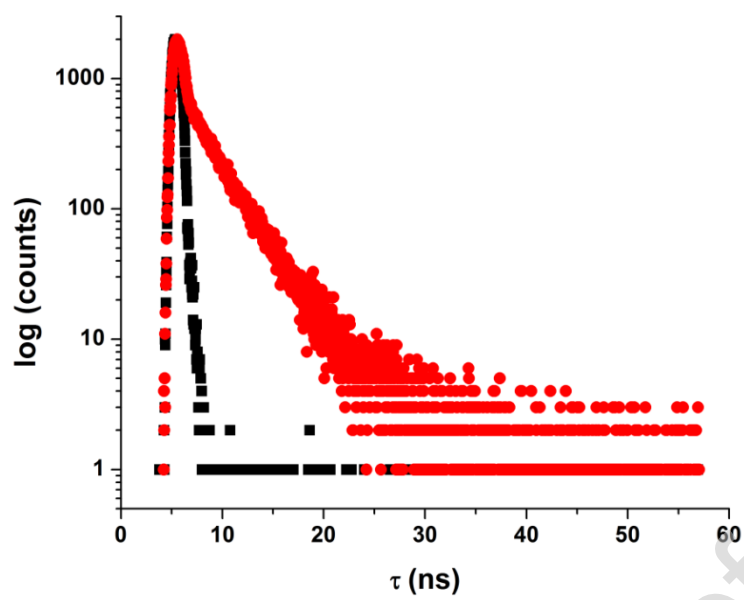


Fig. 3

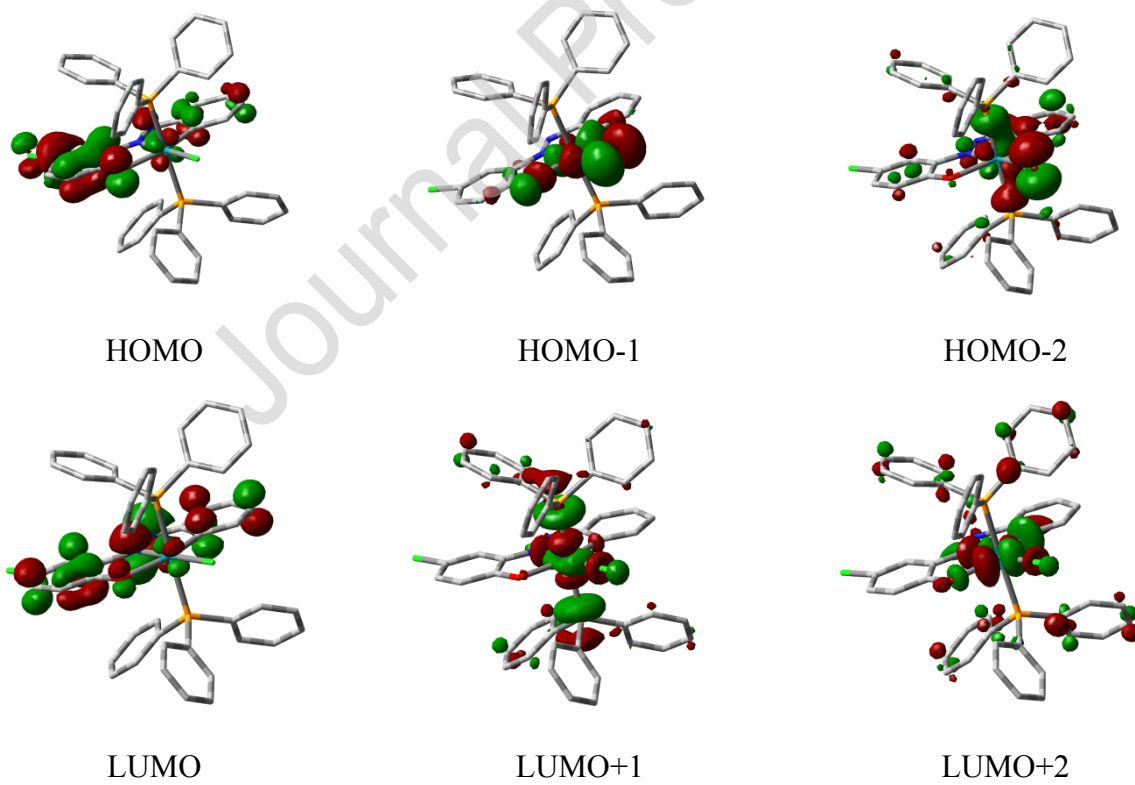


Fig. 4

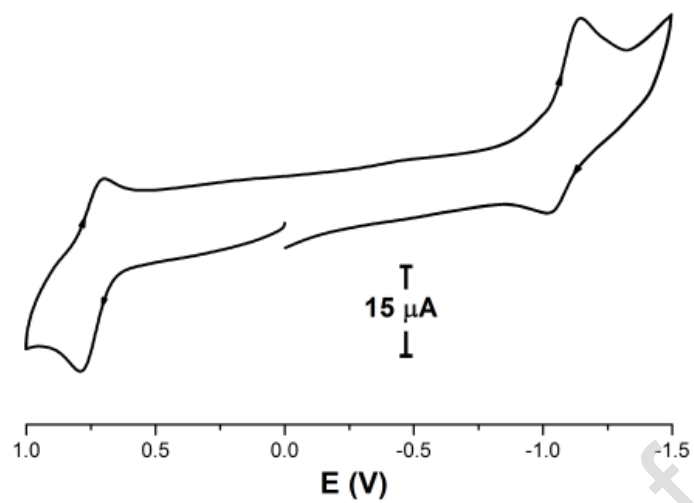


Fig. 5

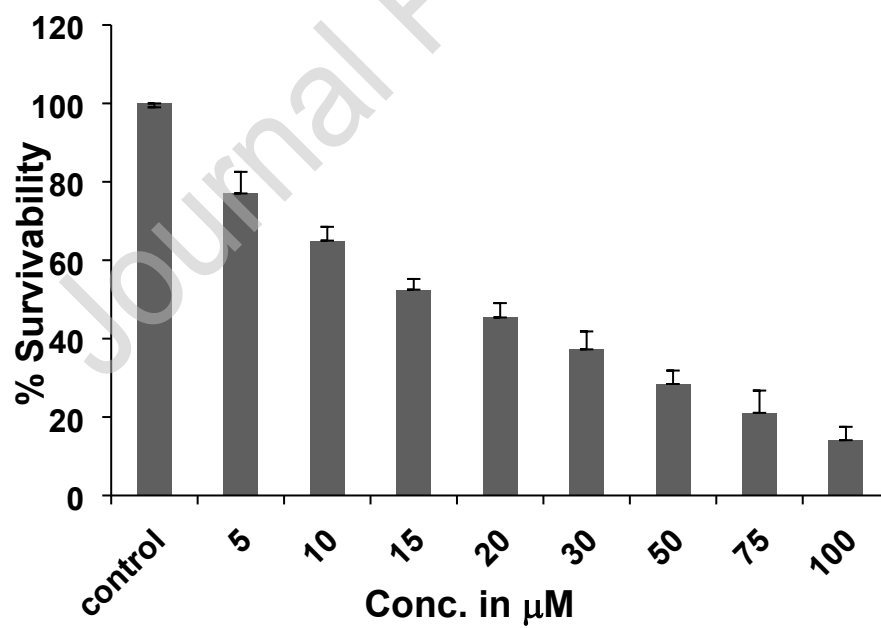


Fig. 6

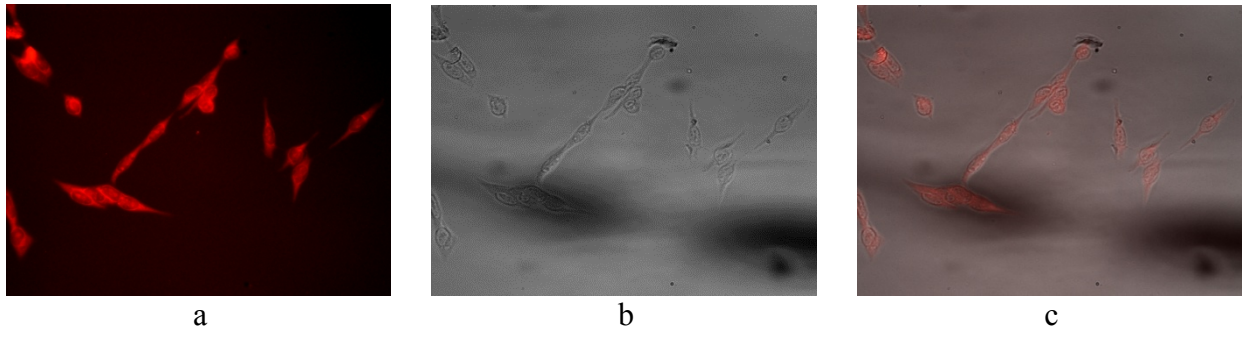


Fig. 7

Journal Pre-proof

There are no conflicts of interest to declare.

Journal Pre-proof

Authors Contribution

Mr. Puspendu Roy designed and synthesized the rhodium(III) cyclometalated complex **1** and performed all the characterization. Mr. Chandan Kumar Manna helped to carry out the catalytic reactions and GC measurements. Dr. Nabendu Murmu, Dr. Deblina Sarkar and Mrs. Paramita Ghosh performed the Cytotoxicity and bio-imaging studies of the complex. Dr. Tapan Kumar Mondal supervised the finding of this work. All authors discussed the results and contributed to the final manuscript.

Journal Pre-proof

HIGHLIGHTS

- New Rh(III) cyclometalated complex, $[\text{Rh}(\text{PPh}_3)_2(\text{L})\text{Cl}]$ (**1**) is synthesized via $\text{sp}^2(\text{C})\text{-S}$ bond activation.
- The pseudo octahedral geometry around rhodium is confirmed by single crystal X-ray diffraction method.
- The complex exhibits low energy emission band at 682 nm with high emission quantum yield ($\phi = 0.103$) upon excitation at 583 nm.
- Cytotoxicity of the complex is studied by MTT method with human breast cancer cell lines and IC_{50} value is found to 18.5 μM .
- In presence of the complex (10 μM) a bright red fluorescence image of MCF-7 cell lines is observed under fluorescence microscope.
- The catalytic activity towards transfer hydrogenation of ketones is studied.